

## Monofunctionalized Au Nanoparticles | Very Important Paper |

## VIP Alkyne-Monofunctionalized Gold Nanoparticles as Massive Molecular Building Blocks

Erich Henrik Peters<sup>[a]</sup> and Marcel Mayor<sup>\*[a,b,c]</sup>

**Abstract:** Using a tripodal, thioether-based ligand comprising a remote protected acetylene, we efficiently stabilize small gold nanoparticles ( $\varnothing \approx 1.2$  nm) which are isolated and purified by chromatography. The 1:1 ligand-to-particle ratio is obtained by comparing the particles' dimensions measured by transmission electron microscopy with the weight fraction of the coating ligand determined by thermogravimetric analysis. The single ligand coating of the gold particle guarantees the presence of a single masked alkyne per particle. It can be addressed by wet chemical protocols providing the particles with the properties

of "massive molecules". The "massive molecule" nature of the particles is demonstrated by involving them in wet chemical coupling protocols like oxidative acetylene coupling providing gold nanoparticle dimers (34 % isolated yield) or alkyne-azide "click"-chemistry with a suitable triazide, giving trimeric particle architectures (30 % determined by transmission electron microscopy). The particle stabilization obtained by the coating ligand allows, for the first time, to treat these multi-particle architectures by size exclusion chromatography.

## Introduction

Colloidal gold has experienced large interest due to its optical and physical properties.<sup>[1–5]</sup> Since the pioneering work by Brust et al.,<sup>[6,7]</sup> various thiol-based organic ligands have been investigated for the stabilization of gold nanoparticles (Au NPs), owing to their synthetic tunability and availability, ease of handling, and favorable stabilization properties. Thiol-stabilized Au NPs were applied in a plethora of fields including catalysis,<sup>[8–10]</sup> sensing and labeling applications,<sup>[11–19]</sup> medical diagnostics and therapeutics<sup>[20–24]</sup> or as building blocks for hybrid materials<sup>[25]</sup> and molecular electronics.<sup>[26–28]</sup> For many of these applications, Au NPs exposing a single functional group, behaving like "massive molecules" enabling their positioning and integration by covalent chemistry are desirable.<sup>[29–32]</sup> Several approaches resulting in monofunctionalized Au NPs stabilized with thiol-based ligands have been reported, including single-


ligand place-exchange reactions on solid support<sup>[33,34]</sup> or in solution, followed by separation by electrophoresis,<sup>[35]</sup> on-Au NP surface polymerization of suitable ligands<sup>[36]</sup> or exchange of the entire ligand shell with carefully tuned thiol mixtures on citrate-stabilized Au NPs.<sup>[37]</sup> Recently, the scope of sulfur-containing ligands for Au NPs has been enhanced towards more complex benzylic thioether-based ligands. The reversible coordinative binding of the thioether to the Au NP surface and the flexible adaptive structure of the multidentate coating ligand holds the promise of efficient and size-selective Au NP passivation. Indeed, oligomeric,<sup>[38–43]</sup> tripodal,<sup>[44–46]</sup> dendrimeric,<sup>[46–50]</sup> and even cage-like<sup>[51]</sup> thioether-based ligands yielded Au NPs with, in some cases, narrow size-distributions, good yields and remarkable stability features. We reported earlier about the favorable Au NP stabilization features of a family of ligands consisting of a central tetraphenylmethane subunit decorated three-fold with multidentate oligomeric chains.<sup>[52]</sup> Particularly appealing were these ligands with tetraphenylmethane-based benzylic thioether oligomers, as in these cases, a single ligand turned out to be able to stabilize an entire Au NP. Interestingly, as only three of the four phenyl units of the central tetraphenylmethane are decorated with an oligomer, the molecular design leaves the fourth phenyl ring upright-standing on the coated Au NP as ideal site for further chemical functionalization.<sup>[53–55]</sup>


Here, we report the successful functionalization of the remaining free phenyl ring by an oligo(phenylene-ethynylene) (OPE) rod exposing a triisopropylsilyl(TIPS)-masked alkyne group. As sketched in Scheme 1, the ligand **1** exposing the OPE rod as a functional group keeps the ability to stabilize an entire Au NP, resulting in monofunctionalized Au NPs which readily undergo chemical reactions in a single position. The combination of a reasonably stable Au NP with a reactive functional group makes these particles addressable by wet chemistry and

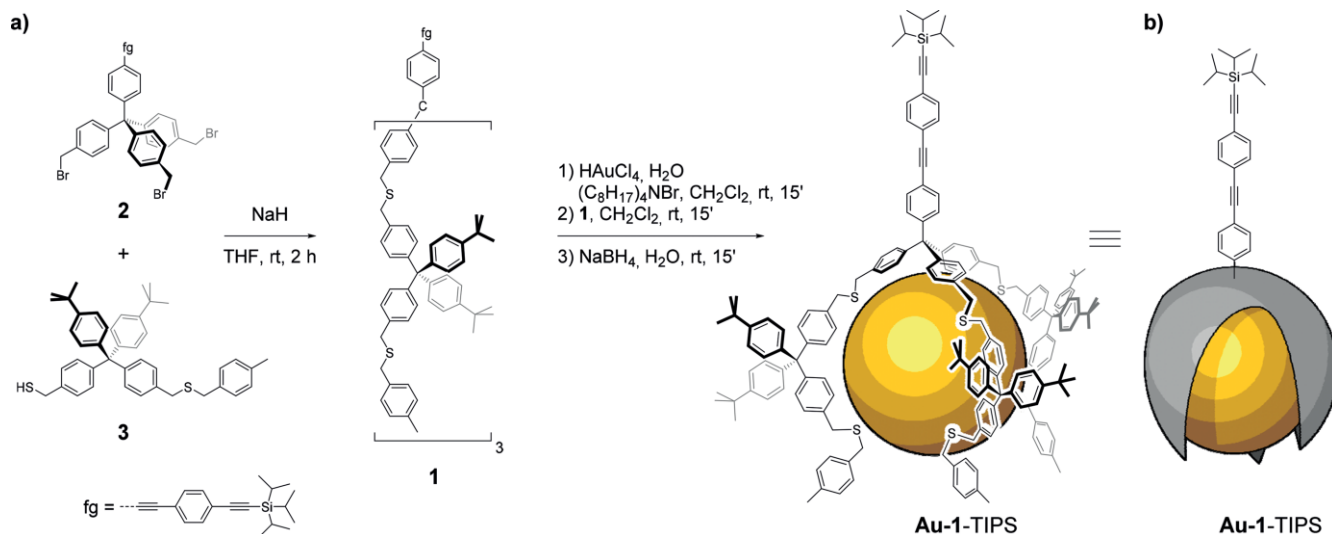
[a] E. H. Peters, Prof. Dr. M. Mayor  
Department of Chemistry, University of Basel,  
St. Johannis-Ring 19, 4056 Basel, Switzerland  
E-mail: marcel.mayor@unibas.ch  
<https://www.chemie1.unibas.ch/~mayor/index.html>

[b] Prof. Dr. M. Mayor  
Institute for Nanotechnology (INT), Karlsruhe Institute of Technology (KIT),  
P. O. Box 3640, 76021 Karlsruhe, Germany  
E-mail: marcel.mayor@kit.edu

[c] Prof. Dr. M. Mayor  
Lehn Institute of Functional Materials (LIFM), Sun Yat-Sen University  
(SYSU),  
Xingang Xi Rd. 135, 510275 Guangzhou, P. R. China

 Supporting information and ORCID(s) from the author(s) for this article are available on the WWW under <https://doi.org/10.1002/ejic.202000273>.

 © 2020 The Authors. Published by Wiley-VCH Verlag GmbH & Co. KGaA. This is an open access article under the terms of the Creative Commons Attribution License, which permits use, distribution and reproduction in any medium, provided the original work is properly cited.



Scheme 1. **a)** Conceptual overview and synthesis of the Au NP exposing a single functional group (fg). **b)** Sketch of the ligand-coated Au NP as massive object exposing a functional group accessible by wet chemistry.

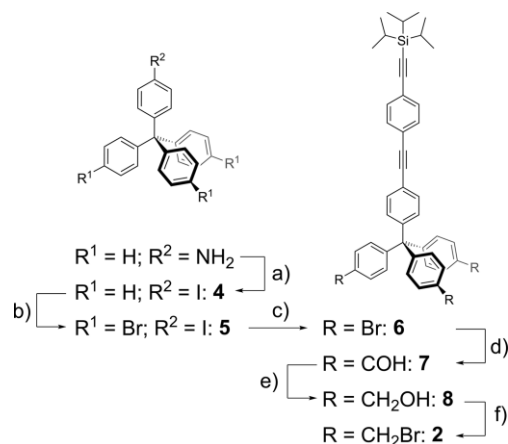
they can be considered as “massive molecules”. The chemical accessibility of the exposed alkyne was demonstrated by standard coupling reactions like oxidative acetylene coupling<sup>[39,41,48]</sup> resulting in “dumbbell”-type dimers and alkyne-azide “click” chemistry<sup>[56,57]</sup> providing Au NP trimers thanks to a suitable triazide linker. Interestingly, the here reported ligand shell stabilizes the Au NP to an extent enabling to expose these small nano-architectures consisting of interlinked Au NPs to size-exclusion chromatography (SEC), which was not the case for previously reported ligand designs.<sup>[39,41,48,49]</sup>

## Results and Discussion

### Ligand Synthesis

The synthesis of tripodal ligand **1** is shown in Scheme 1. The three benzylic bromides of precursor **2** were substituted with a moderate excess of thiol **3** (1.23 equivalents per bromide), using sodium hydride (NaH) as a base in freshly distilled tetrahydrofuran (THF). After aqueous work-up, the ligand was isolated in 55 % yield by silica plug filtration and automated gel permeation chromatography (GPC, in chloroform).

The synthesis of the central linking unit was performed in six steps with an overall yield of 54 % (Scheme 2). Precursor **4** was obtained via Sandmeyer-type reaction applied to 4-tritylaniline in good 80 % yield. Subsequent treatment with bromine gave the tribromide **5** quantitatively. Profiting from the improved reactivity of the iodine substituent in palladium-catalyzed coupling reactions,<sup>[58]</sup> the OPE-rod exposing the TIPS-protected alkyne was introduced via Sonogashira cross-coupling reaction performed at room temperature, providing the OPE-rod **6** exposing three terminal *para*-bromophenyls. Threefold lithium-halogen exchange was achieved with *tert*-butyl-lithium in  $-78^\circ\text{C}$  cold THF, and quenching with *N,N*-dimethylformamide (DMF) gave the trialdehyde **7** in excellent 88 % yield after aqueous work-up and column chromatography. The three aldehydes were quantitatively reduced to benzylic alcohols in **8** with so-



Scheme 2. Synthesis of functionalized central linking unit **2**. a) 1)  $\text{BF}_3\text{Et}_2\text{O}$ ,  $\text{CH}_2\text{Cl}_2$ ,  $-10^\circ\text{C}$ , 45', 2)  $t\text{BuONO}$ ,  $\text{CH}_2\text{Cl}_2$ ,  $-10^\circ\text{C}$ , 45', 3)  $\text{I}_2$ ,  $\text{KI}$ ,  $-10^\circ\text{C}$  to r.t., 15 h, 80 %; b)  $\text{Br}_2$ , neat, r.t., 30', quant.; c)  $\text{Pd}(\text{PPh}_3)_2\text{Cl}_2$ ,  $\text{TIPSC}\equiv\text{C}-p\text{C}_6\text{H}_4-\text{C}\equiv\text{CH}$ ,  $\text{CuI}$ ,  $\text{Et}_3\text{N}$ ,  $\text{CH}_2\text{Cl}_2$ , r.t., 2 h, 76 %; d) 1)  $t\text{BuLi}$ , THF,  $-78^\circ\text{C}$ , 2 h, 2) DMF,  $-78^\circ\text{C}$  to r.t., 2 h, 88 %; e) 1)  $\text{NaBH}_4$ , MeOH,  $0^\circ\text{C}$ , 2 h, 2)  $\text{HCl}$  (aq.),  $0^\circ\text{C}$ , r.t., quant.; f)  $\text{CBr}_4$ ,  $\text{PPh}_3$ ,  $\text{CH}_2\text{Cl}_2$ ,  $-10^\circ\text{C}$ , 1 h quant.

dium borohydride. Finally, in a threefold Appel-reaction, the benzylic alcohols were converted into the benzylic bromides of **2** quantitatively.

The assembly of the terphenylmethane building block **3** exposing a benzylic thiol was achieved following a previously published protocol.<sup>[42]</sup>

All new compounds were characterized by  $^1\text{H}$ - and  $^{13}\text{C}$ -NMR spectroscopy and high-resolution mass spectrometry.

### Au NP Synthesis

The Au NPs stabilized by ligand **1** were synthesized following a previously published protocol<sup>[38]</sup> based on a variation of the Au NP synthesis proposed by *Brust* et al.<sup>[6]</sup> In the aqueous phase of a biphasic system, one equivalent of gold salt ( $\text{HAuCl}_4$ ) for each sulfur atom in the ligand, i.e. 6 equivalents, was added.

The transfer of the gold salt from the aqueous to the organic phase was achieved by addition of tetra-*n*-butyl ammonium bromide (TOAB, 2 equivalents with respect to HAuCl<sub>4</sub>, i.e. 12 equivalents) to the organic phase. The ligand was added dissolved in CH<sub>2</sub>Cl<sub>2</sub>. Nucleation of the Au NPs was induced via reduction by aqueous NaBH<sub>4</sub> (8 equivalents with respect to HAuCl<sub>4</sub>, i.e. 48 equivalents). Upon addition of the reducing agent, an immediate color change of the organic phase from bright orange to opaque dark brown was observed. After rigorous stirring for 15 min, the organic phase was separated and concentrated in a N<sub>2</sub> stream to prevent possible thermal aggregation of NPs. Precipitation of the Au NPs from the concentrated organic solution was achieved by addition of ethanol. Repeated centrifugation and subsequent SEC provided pure samples of the Au NPs without remaining traces of ligand molecules or TOAB. The colloidal gold particles stabilized by ligand **1** are labeled as **Au-1-TIPS** and were isolated in excellent yields above 95 %. **Au-1-TIPS** was the only detectable form of gold throughout the synthesis and the mass losses were due to the handling during the purification procedures.

### Au NP Analysis and Characterization

The Au NPs were characterized by variable temperature UV/Vis absorption spectroscopy, transmission electron microscopy

(TEM), and thermogravimetric analysis (TGA). Finally, the “molecule-like” behavior of **Au-1-TIPS** was demonstrated by engaging them in wet chemistry coupling protocols producing small nano-architectures like dimers and trimers which could be detected by TEM.

The UV/Vis absorption spectrum of **Au-1-TIPS** (Figure 1c) displays discrete bands between 300–350 nm, characteristic for the absorbance of the OPE subunit of the ligand **1**. Apart from these features, the continuous increase towards shorter wavelength without a surface plasmon band points at Au NPs with diameters below 2 nm. Only with Au NPs of dimensions below 2 nm, the rate of surface scattering exceeds the rate of bulk scattering and the electron-donating character of the coordinating sulfur atoms of the coating ligand increases the surface electron density significantly, reflected in a broadening of the surface plasmon band.<sup>[59]</sup> It is noteworthy that very similar optical behavior was reported for the parent ligand structure without the exposed functional group.<sup>[52]</sup> The OPE subunit of **1** acts as an optical label and the very comparable absorption of the OPE subunit of **Au-1-TIPS** compared with the free ligand **1** not only proves the presence of the ligand on the Au NP, but also supports the hypothetical picture of an exposed and dissolved OPE rod which does not interfere with the Au NP surface. The dimensions of the Au NPs were further analyzed by TEM (Fig-

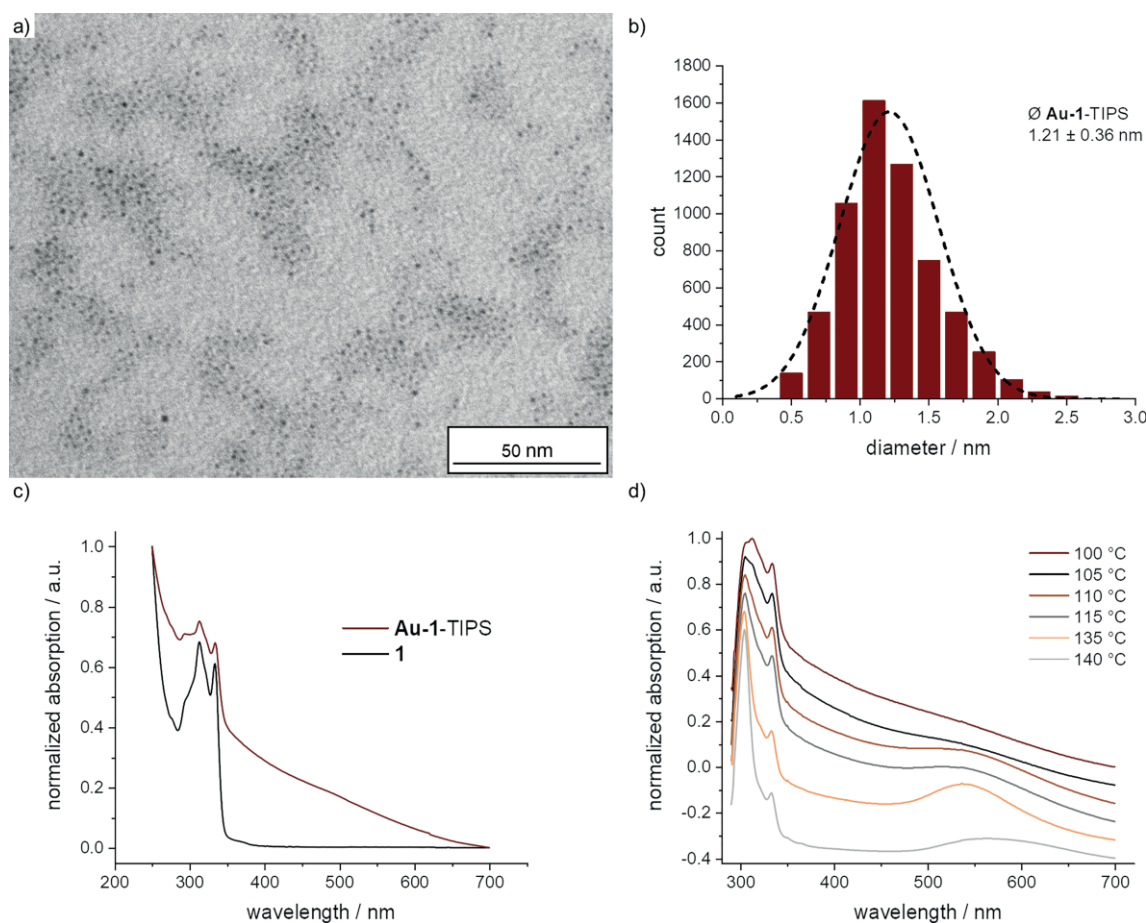


Figure 1. **a)** TEM micrograph of **Au-1-TIPS**; **b)** size-distribution of **Au-1-TIPS** obtained from TEM micrographs; **c)** UV/Vis absorption spectrum of **Au-1-TIPS** in comparison with ligand **1**; **d)** UV/Vis absorption spectra at selected temperatures, offset for clarity.

ure 1a–b) and the recorded diameters of  $1.21 \pm 0.36$  nm confirmed the initial claims derived from the UV/Vis experiments. The Au NP size distribution was determined with TEM micrographs comprising more than 6000 NPs, using the threshold and particle analysis tools from ImageJ.<sup>[60]</sup>

TGA of **Au-1-TIPS** revealed a mass loss of 19.0 % between 200 and 600 °C which was attributed to the combustion of the coating organic ligand **1**. Assuming a spherical shape, the Au NP diameter of 1.21 nm determined by TEM allowed to determine the Au NP's volume ( $0.93 \text{ nm}^3$ ). With the density of gold ( $19.32 \text{ g cm}^{-3}$ ), the mass of an average Au NP was determined to be  $1.79 \times 10^{-20}$  g, and, by multiplication with *Avogadro's* number ( $N_A$ :  $6.022 \times 10^{23} \text{ mol}^{-1}$ ), the molecular weight of the average uncoated Au NP was determined to be  $10792 \text{ g mol}^{-1}$ . The molecular weight of the ligand **1** with the formula  $\text{C}_{176}\text{H}_{188}\text{S}_6\text{Si}$  is  $2523.89 \text{ g mol}^{-1}$ . The molecular weight of the proposed particle **Au-1-TIPS** coated by a single ligand is, with  $13316 \text{ g mol}^{-1}$ , the sum of both. The weight contribution of the coating ligand **1** fits, with 18.95 %, perfectly the weight loss recorded during TGA (19.0 %), corroborating the claim that a single ligand **1** is coating and stabilizing an entire Au NP. The same issue is examined in Table 1 displaying that the same number of gold atoms per particle is obtained from the TGA and the TEM analysis.

The Au NPs **Au-1-TIPS** coated with a single ligand exposing an OPE rod can be regarded as “massive molecules” with a peripheral TIPS-protected alkyne as functional group. To explore the stability of this “massive molecule” and thus also the scope of potential reaction conditions, samples of **Au-1-TIPS** were dispersed in *ortho*-xylene and gradually heated while their optical features were monitored by UV/Vis spectroscopy. Applying a heating gradient of 10 °C per hour, the UV/Vis spectra of the sample remained unchanged up to 105 °C (Figure 1d). Above this temperature, the samples turned red and the emergence of a plasmon band in the UV/Vis was observed. Upon extended exposure to temperatures above 105 °C, decoloration of the sample due to precipitation was observed. The thermal decomposition of **Au-1-TIPS** above 105 °C is interpreted as agglomeration to larger particles, either due to too violent collisions for the delicate steric protection provided by coating **1** or due to prior thermal detachment of **1**. It is noteworthy that a comparable decomposition temperature was observed for the parent ligand structure (110 °C),<sup>[52]</sup> documenting further the separation between the coating ligand subunit of **1** and the attached OPE rod.

After the determination of the thermal stability of **Au-1-TIPS**, its potential as precursor in wet-chemical reactions as building block for nano-architectures was explored.

### Au-1-TIPS as Precursor in Coupling Reactions I: Dimerization

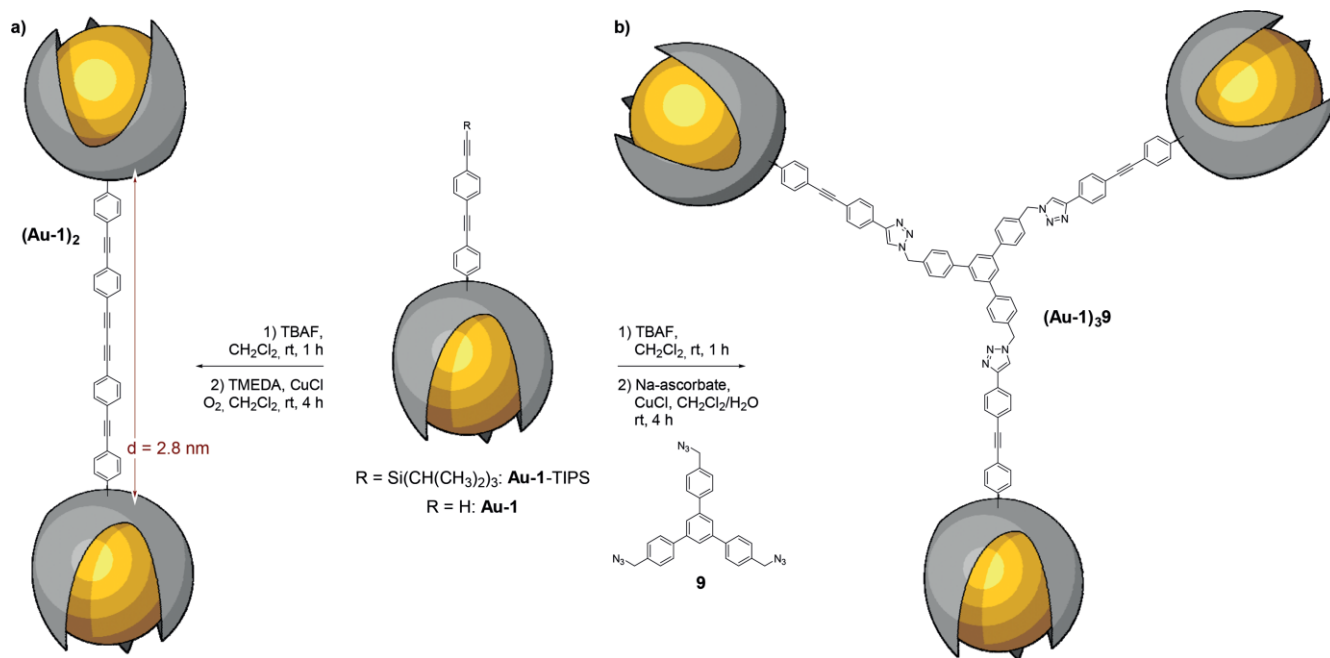
The analytical data of **Au-1-TIPS** displayed a Au NP coated by a single ligand and, consequently, also only one OPE rod per Au NP. Furthermore, the comparison of the UV/Vis spectra of **Au-1-TIPS** and the free ligand **1** suggested an entirely dissolved and thus wet-chemically addressable OPE subunit exposed at the Au NP surface. The OPE rod exposes a TIPS-protected terminal alkyne as masked but reactive functional group which can be involved e.g. in various coupling protocols. To demonstrate the engagement of **Au-1-TIPS** as “massive molecule” in coupling chemistry, the TIPS-masked alkyne was deprotected profiting from the fluoride ions of tetra-*n*-butylammoniumfluoride (TBAF) in  $\text{CH}_2\text{Cl}_2$  (Scheme 3). After aqueous work-up, the deprotected Au NPs were exposed to typical *Glaser-Hay* oxidative acetylene coupling conditions.<sup>[61,62]</sup> They were re-dissolved in  $\text{CH}_2\text{Cl}_2$  and  $\text{Cu}^{(II)}$  ions were added together with *N,N,N',N'*-tetramethylethane-1,2-diamine (TMEDA) as ligand dissolving the copper ion. The reaction was vigorously stirred at ambient air to guarantee the presence of dissolved oxygen. To avoid aggregation of the coated gold particles, the reaction was kept for 4 hours at room temperature. After aqueous work-up and subsequent repetitive separation by SEC using  $\text{CH}_2\text{Cl}_2$  and toluene as eluent, Au NP dimers [**Au-1**]<sub>2</sub> were isolated in 34 % yield. It is noteworthy that these dimeric Au NP architectures based on the ligand **1** were the first larger systems resisting decomposition on the SEC column, documenting further the superior stability of Au NP coated by the ligand **1**. All our earlier ligand designs based on benzylic thioethers survived SEC conditions as monomers, but the resulting interlinked NP architectures disintegrated when exposed to the shear forces of SEC.<sup>[39,41,48]</sup>

The yield of [**Au-1**]<sub>2</sub> was also determined by analyzing TEM micrographs of the crude reaction mixture. The reaction mixture was diluted to an extent avoiding the agglomeration of Au NPs on the TEM grid. 53 micrographs (each 340 nm × 260 nm) comprising a total of 2077 Au NPs were analyzed, covering  $4.69 \mu\text{m}^2$  of the TEM grid. Pairs of Au NPs with a spacing up to 3.2 nm were considered as [**Au-1**]<sub>2</sub>. With 826 of 2077 NPs being part of a dimer corresponding to a yield of 39.8 %, the TEM analysis confirmed the yield isolated by SEC.

Table 1. Ligand-to-gold ratio of **Au-1-TIPS**. The number of gold atoms of an average particle is calculated from the TGA data (top) and from the dimension of the NP determined by TEM (bottom). *m*(**1**): mass loss due to burned ligand **1**; *M*(**1**): molar mass of **1**; *n*(**1**): number of mol of ligand **1**; *m*<sub>Au</sub>: mass of remaining gold; *n*<sub>Au</sub>: number of mol of gold; *n*<sub>Au</sub>/*n*(**1**): average number of gold atoms per ligand according to the TGA data;  $\varnothing_{\text{NP}}$ : diameter of an average NP determined by TEM; *V*<sub>NP</sub>: volume of the NP =  $4/3\pi r^3$ ; *m*<sub>NP</sub>: mass of the NP =  $V_{\text{NP}} \cdot \rho_{\text{Au}}$  (with  $\rho_{\text{Au}} = 19.32 \text{ g cm}^{-3}$ ); *M*<sub>Au</sub>: molar mass of gold ( $196.97 \text{ g mol}^{-1}$ ); *n*<sub>Au</sub>: number of mol of gold =  $m_{\text{NP}}/M_{\text{Au}}$ ; *n*<sub>Au</sub>/*NP*: average number of gold atoms per NP =  $n_{\text{Au}} \cdot N_A$  ( $N_A = 6.022 \times 10^{23} \text{ mol}^{-1}$ ).

<b>Au-1-TIPS</b>	<i>m</i> ( <b>1</b> ) [mg]	<i>M</i> ( <b>1</b> ) [g/mol]	<i>n</i> ( <b>1</b> ) [mol]	<i>m</i> <sub>Au</sub> [mg]	<i>n</i> <sub>Au</sub> [mol]	<i>n</i> <sub>Au</sub> / <i>n</i> ( <b>1</b> )
TGA	0.545	2523.9	$2.18 \times 10^{-7}$	2.33	$1.18 \times 10^{-5}$	54.7
	$\varnothing_{\text{NP}}$ [nm]	<i>V</i> <sub>NP</sub> [nm <sup>3</sup> ]	<i>m</i> <sub>NP</sub> [g]	<i>M</i> <sub>Au</sub> [g/mol]	<i>n</i> <sub>Au</sub> [mol]	<i>n</i> <sub>Au</sub> / <i>NP</i>
TEM	$1.21 \pm 0.36$	0.928	$1.79 \times 10^{-20}$	196.97	$9.1 \times 10^{-23}$	54.8





Scheme 3. Nano-architectures obtained by using **Au-1-TIPS** as starting materials. **a**) Dimerization by oxidative acetylene coupling. **b**) Trimerization profiting from alkyne-azide "click"-chemistry.

Additional structural features of **(Au-1)<sub>2</sub>** were extracted from TEM micrographs (Figure 2a). The size-distribution of the Au NPs after the coupling reaction (Figure 2b) resembles, with  $1.18 \pm 0.29$  nm, within the limits of the method, the one recorded for the parent sample **Au-1-TIPS**. This suggests that, during the entire deprotection-homocoupling protocol, the Au NPs remain stable and protected by the coating ligand, corroborating the "massive molecule" behavior of **Au-1-TIPS** in the reaction sequence.

TEM micrographs of the isolated, "dumbbell-like" Au NP dimers (Figure 2a) enabled to analyze the inter-NP distances in more details. Interestingly, the distribution of the NP spacing clearly displayed two maxima (Figure 2c). The majority of about 80 % of the recorded Au-NP distances was, with  $2.62 \pm 0.21$  nm, in the dimensions of the diethynyl-linker expected as product of the oxidative acetylene coupling, as the distance for the fully stretched linker estimated by simple MM2 simulation was 2.8 nm (distance between both tertiary methane carbon atoms of the rod-terminating tetraphenylmethane subunits, see Scheme 3a). In principle, any shorter distance might be attributed to the projection of the Au NPs of a "dumbbell" dimer not lying flat on the TEM grid. For such an explanation, one would, however, rather expect a continuous tailing to shorter distances and not a discrete maximum. Thus, in similarity to "dumbbell" architectures based on dendrimer-coated Au-NPs,<sup>[48]</sup> the shorter inter-NP distance of  $1.64 \pm 0.20$  nm (recorded for about 20 %) most likely points at direct coordinative contacts between an Au NP and the terminal acetylene exposed by the OPE rod of the deprotected **Au-1**.<sup>[63]</sup> Such a coordination between alkyne and Au NP requires access to the Au NP surface, showing that the ligand **1** is not covering the entire surface of

the stabilized Au NP in **Au-1**. Interestingly, trimeric structures e.g. consisting of "dumbbell"-type dimers formed by oxidative acetylene coupling with one of its terminal Au NPs engaged in a coupling with the terminal acetylene of a third deprotected **Au-1** were, with only 4 observed cases, too rare to exclude random arrangements on the TEM grid. The Au NP dimers with short spacing are of comparable stability to the longer ones and do also not decompose during the SEC process. Also, we were not able to distinguish both structures during the SEC experiment, which was not surprising, considering the working hypothesis that both structures exclusively differ in the inter-linking of two **Au-1**-type subunits.

### Au-1-TIPS as Precursor in Coupling Reactions II: Trimerization

The lack of trimers observed in the homocoupling protocol discussed above raised the question if there could be an intrinsic limitation disqualifying trimerization. As alternative approach to couple three Au NPs to a trimeric nano-architecture, alkyne-azide "click"-chemistry has already been applied successfully for dendrimer-stabilized Au NPs.<sup>[49]</sup> Thus, a sample of **Au-1-TIPS** was deprotected and the liberated alkynes were exposed to a "click" protocol with the triazide 1,3,5-tris[*p*-(azidomethyl)phenyl]benzene (**9** in Scheme 3) as threefold central coupling unit. To the deprotected **Au-1** dissolved in CH<sub>2</sub>Cl<sub>2</sub>, the triazide **9** was added and, while vigorously stirring, aqueous solutions of copper sulfate and sodium ascorbate as reducing agent were added (Scheme 3b). To avoid aggregation of the coated gold particles, the reaction was kept for 4 hours at room tempera-

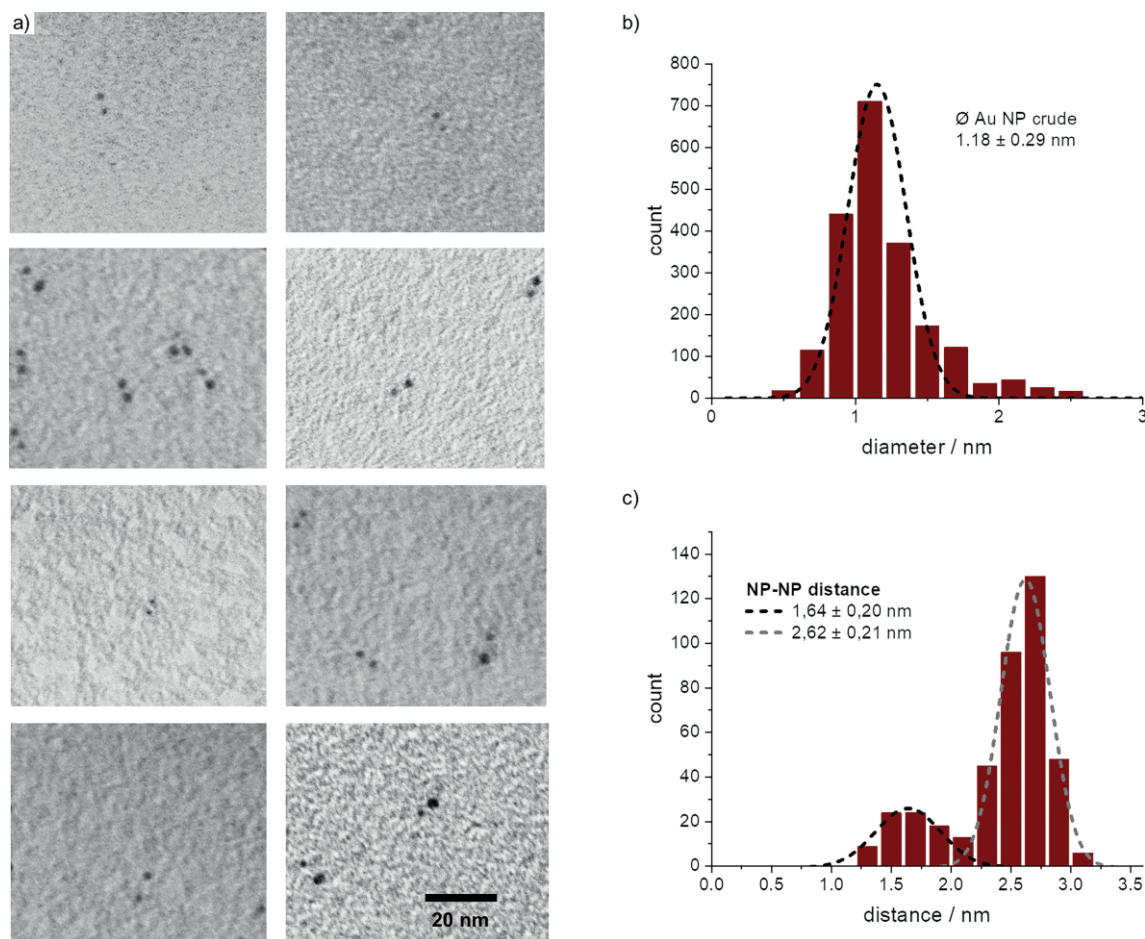


Figure 2. “Dumbbell”-type dimers formed by exposing **Au-1-TIPS** to a deprotection–homocoupling protocol. **a**) TEM micrographs of **(Au-1)<sub>2</sub>** (scale bar is valid for all 8 micrographs). **b**) Size-distribution of Au NPs after the deprotection–homocoupling protocol. **c**) Distribution of the interparticle distance in **(Au-1)<sub>2</sub>**.

ture. After extraction with  $\text{CH}_2\text{Cl}_2$ , the composition of the crude reaction mixture was analyzed by TEM. 42 micrographs (each  $340 \times 260$  nm) comprising a total of 1587 Au NPs were analyzed, covering  $3.71 \mu\text{m}^2$  of the TEM grid. Groups of 3 NPs with a maximal separation smaller than 4.5 nm were considered as the trimeric **(Au-1)<sub>3</sub>9**. The slightly larger accepted radius compared with the homocoupled **(Au-1)<sub>2</sub>** is due to both the larger dimensions and the increased flexibility of the particle-interlinking organic structure. From the 1587 NPs, 477 NPs or 30.1 % were engaged in a **(Au-1)<sub>3</sub>9** structure, 324 NPs or 20.4 % were observed as dimers of Au NPs, and 786 NPs or 49.5 % were recorded as monomers. Whether the dimers are formed due to only twofold “click”-chemistry-type coupling to **9**, or to homocoupled **(Au-1)<sub>2</sub>**, cannot be distinguished in the TEM micrographs.

Also for the “click”-chemistry protocol, a very comparable size-distribution (Figure 3b,  $1.28 \pm 0.30$  nm) of the Au NPs after the coupling reaction was observed, pointing at the integrity of **Au-1** during the applied reaction conditions. In analogy to the homocoupled **(Au-1)<sub>2</sub>**, also **(Au-1)<sub>3</sub>9** survived SEC conditions. However, while fractions comprising **(Au-1)<sub>3</sub>9** and the di-

meric Au NP architectures could be separated from the monomeric Au NPs, the method failed to isolate pure **(Au-1)<sub>3</sub>9** fractions.

TEM micrographs of **(Au-1)<sub>3</sub>9** (Figure 3a) enabled the analyses of the interparticle distances (Figure 3c). The rather broad and unspecific distance distribution reflects the increased structural variety in the arrangement of the three Au NP in **(Au-1)<sub>3</sub>9**, due to the flexibility of the interlinking scaffold comprising triazole subunits attached at benzylic positions.

While the spatial grouping of Au NPs by TEM analyses of the reaction mixtures support for both coupling reactions the formation of the desired oligo-NP nano-architectures, the method does not comprise any further chemical information. As example, an interesting chemical issue was the rather moderate yield of the desired oligo-NP objects with 39.8 % for **(Au-1)<sub>2</sub>** and 30.1 % for **(Au-1)<sub>3</sub>9** respectively. Whether these moderate yields reflect the lack of reactivity of the “massive molecule” **Au-1** in the coupling reaction or, in the step before, an incomplete deprotection of **Au-1-TIPS** cannot be distinguished by the here reported studies.

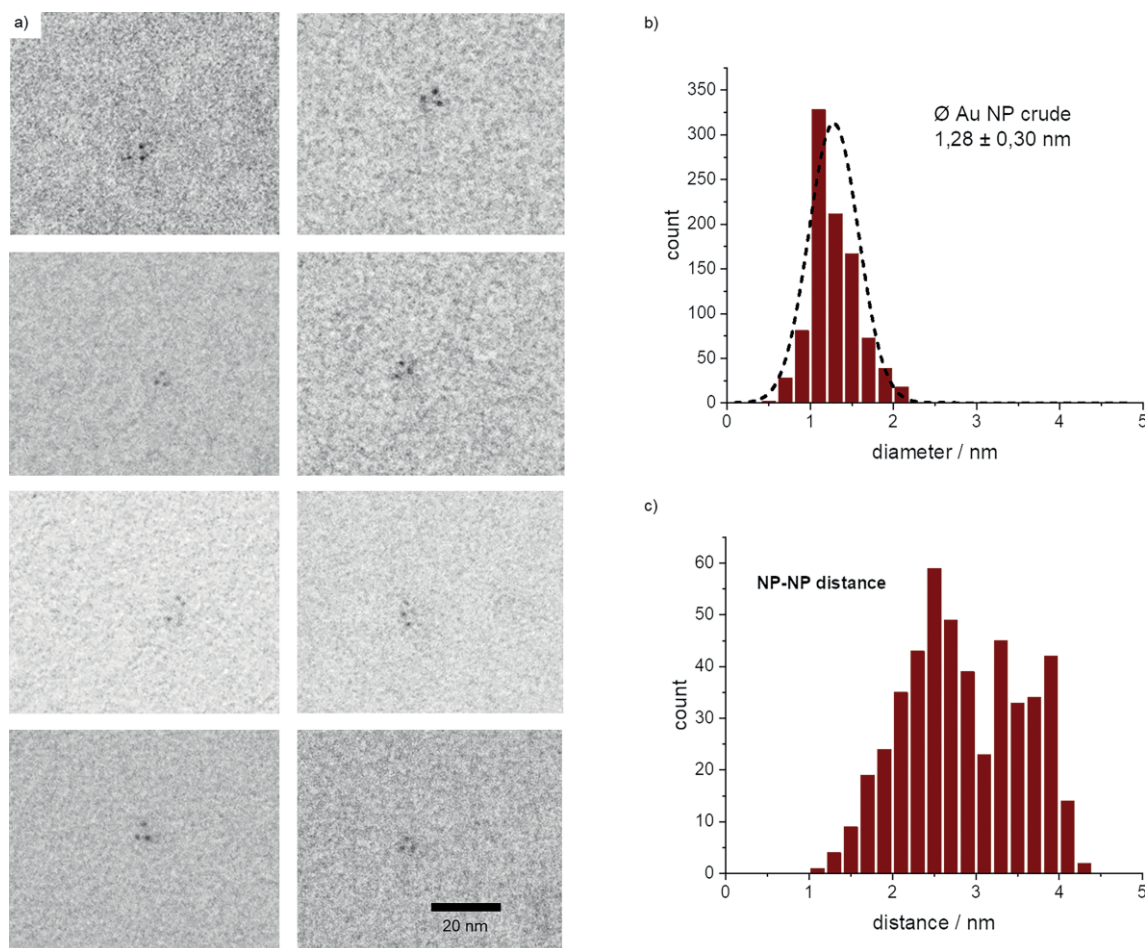


Figure 3. TEM analyses of **(Au-1)<sub>39</sub>**. **a)** TEM micrographs of **(Au-1)<sub>39</sub>** (scale bar is valid for all 8 micrographs). **b)** Size-distribution of Au NPs after the deprotection–“click”–coupling protocol. **c)** Distribution of the interparticle distance in **(Au-1)<sub>39</sub>**.

## Conclusion

In summary, a new ligand for the efficient and controlled synthesis of monofunctionalized Au NPs combining the massive nature of the particles with the wet chemical addressability of a molecule and thus behaving as “massive molecules” with superior stability properties is reported. The ligand design is based on a central tetraphenylmethane subunit unifying three oligomeric benzyl sulfide chains forming the Au NP-stabilizing subunit and exposing a masked alkyne on an OPE rod attached to the fourth phenyl ring of the central unit. Au NPs with narrow size distribution around 1.2 nm coated by a single ligand are obtained efficiently and display very good stability features, withstanding decomposition up to 105 °C in dispersion. The “massive molecule”-like behavior is displayed by deprotecting the terminal alkyne of the coated Au NP and engaging it in coupling protocols providing interlinked dimeric and trimeric Au NP systems as displayed by TEM analyses. With the here reported coating ligand, the particles of these nano-architectures are stable enough to resist the shear forces during purification by SEC.

We are currently investigating the catalytic activity of these ligand-coated Au NPs and explore their scope as labels in proteins and even larger biological systems.

## Experimental Section

### Materials

All commercially available starting materials were of reagent grade and used as received, unless stated differently. Absolute THF was purchased from Acros, stored over 4 Å molecular sieves, pre-dried with CaH, handled under argon and freshly distilled from sodium before each use. Pure CH<sub>2</sub>Cl<sub>2</sub> was purchased from J. T. Baker. Pure toluene was purchased from Acros. Pure DMF was purchased from Acros Organics. *tert*-butylmethyl ether (TBME), *c*-hexane, ethyl acetate (EtOAc), and CH<sub>2</sub>Cl<sub>2</sub> from Biosolve were used for purification and were of technical grade. Column chromatography was carried out on SiliaFlash P60 (particle size 40–63 μm) from SiliCycle. SEC for the purification of Au NPs mono-, di- and trimers was performed manually using Bio-Rad Bio-Beads S-X1 (operating range 600–14 000 g mol<sup>-1</sup>) with CH<sub>2</sub>Cl<sub>2</sub> or toluene as eluent. Deuterated solvents were purchased from Cambridge Isotope Laboratories.

### Equipment and Measurements

<sup>1</sup>H- and <sup>13</sup>C-NMR spectra were recorded with a Bruker DPX 400 instrument (<sup>1</sup>H resonance 400 MHz, <sup>13</sup>C resonance 101 MHz) or a Bruker DRX 500 instrument (<sup>1</sup>H resonance 500 MHz, <sup>13</sup>C resonance 126 MHz) at 298 K. The chemical shifts (δ) are reported in ppm and are referenced to the residual proton signal of the deuterated solvent ([D]chloroform: 7.26 ppm) for <sup>1</sup>H spectra or the carbon of the solvent ([D]chloroform: 77.1 ppm) for <sup>13</sup>C spectra. The coupling con-



stants (*J*) are given in Hertz (Hz), the multiplicities are denoted as s (singlet), d (duplet), t (triplet), m (multiplet), and br (broad). High-resolution mass spectra (HRMS) were measured as HR-ESI-ToF-MS with a Maxis 4G instrument from Bruker or a Bruker UltraFlex II – MALDI-ToF-MS. For purification of the ligands, a (automated) Shimadzu Prominence System was used with SDV preparative columns from Polymer Standards Service (two Showdex columns in series, 20 mm × 600 mm each, exclusion limit: 30 000 g mol<sup>-1</sup>) with chloroform as eluent. UV/Vis measurements were recorded on a Jasco V-770 spectrophotometer using 117.100F-QS cuvettes from Hellma Analytics (10 mm light path). TEM was performed on a Philips CM100 TEM at 80 kV using copper grids (Cu-400HD) from Pacific Grid Tech. TGA was measured on a Mettler Toledo TGA/SDTA851<sup>e</sup> with a heating rate of 10 °C min<sup>-1</sup>.

**p-Iodophenyltriphenylmethane (4):**<sup>[64]</sup> To a degassed 250 mL two-neck flask equipped with rubber septum and thermometer, BF<sub>3</sub>OEt<sub>2</sub> (3.67 mL, 29.0 mmol, 2 equiv.) was added and cooled to -10 °C. In a separate flask, 4-tritylaniline (5.01 g, 14.5 mmol, 1 equiv.) was dissolved in 100 mL of degassed CH<sub>2</sub>Cl<sub>2</sub> and was added dropwise via transfer cannula. The mixture was stirred at -10 °C for 45 minutes after which time *t*BuNO<sub>2</sub> (3.00 mL, 25.0 mmol, 1.75 equiv.) dissolved in 50 mL of degassed CH<sub>2</sub>Cl<sub>2</sub> was added dropwise via transfer cannula. The mixture was stirred at -10 °C during 45 minutes. I<sub>2</sub> (4.78 g, 18.9 mmol, 1.3 equiv.) and KI (3.61 g, 21.8 mmol, 1.5 equiv.) were added to the mixture which was thereafter stirred vigorously during 15 h and allowed to slowly warm up to r.t. Excess halogen was quenched upon addition of saturated aqueous Na<sub>2</sub>S<sub>2</sub>O<sub>3</sub>. After phase separation, the aqueous phase was extracted twice more with CH<sub>2</sub>Cl<sub>2</sub> and dried with Na<sub>2</sub>SO<sub>4</sub>. After evaporation of the volatile in vacuo, compound **4** was purified by column chromatography (c-hexane) as a pale solid (5.2 g, 11.6 mmol, 80 %). <sup>1</sup>H-NMR (400 MHz, [D]Chloroform): δ = 7.60–7.55 (m, 2H), 7.25–7.20 (m, 6H), 7.20–7.17 (m, 6H), 7.17–7.15 (m, 3H), 7.00–6.96 (m, 2H).

**p-Iodophenyltri(p-bromophenyl)methane (5):**<sup>[65]</sup> In a 250 mL flask, **4** (4.91 g, 11.0 mmol, 1 equiv.) was dissolved in Br<sub>2</sub> (20 mL, 385 mmol, 35 equiv.) and stirred at r.t. for 30 minutes. The reaction was diluted with CH<sub>2</sub>Cl<sub>2</sub> and crushed ice was added. The mixture was further cooled with an ice bath and saturated aqueous Na<sub>2</sub>S<sub>2</sub>O<sub>3</sub> was slowly added until all the excess bromine was quenched. The mixture was extracted twice with CH<sub>2</sub>Cl<sub>2</sub>, dried with Na<sub>2</sub>SO<sub>4</sub>, and the volatile evaporated in vacuo. The crude was subjected to silica plug filtration (CH<sub>2</sub>Cl<sub>2</sub>) and recrystallized from hot c-hexane to yield **5** as a pale solid (7.51 g, 11.0 mmol, quant.). <sup>1</sup>H-NMR (400 MHz, [D]Chloroform): δ = 7.63–7.57 (m, 2H), 7.41–7.37 (m, 6H), 7.04–6.99 (m, 6H), 6.92–6.84 (m, 2H).

**p-[p-(Triisopropylsilylethynyl)phenylethynyl]phenyltri(p-bromophenyl)methane (6):** In a dry, degassed 100 mL flask, **5** (1.4 g, 2.05 mmol, 1 equiv.), bis(triphenylphosphine)palladium(II)chloride (0.24 g, 0.205 mmol, 0.1 equiv., cat.) and CuI (0.195 g, 1.03 mmol, 0.5 equiv., cat.) were dissolved in 40 mL of CH<sub>2</sub>Cl<sub>2</sub> and 10 mL of triethylamine (71.2 mmol, 35 equiv.). The mixture was bubbled with Ar for 20 minutes after which time, *p*-(triisopropylsilylethynyl)phenylethyne (1.16 g, 4.1 mmol, 2 equiv.) was added portionwise while stirring for 2 hours at r.t. The solvent was then evaporated in vacuo and the crude subjected to column chromatography (c-hexane 10:1 CH<sub>2</sub>Cl<sub>2</sub>) to afford **6** as a yellow foam (1.3 g, 1.55 mmol, 76 %). <sup>1</sup>H-NMR (400 MHz, [D]Chloroform) δ = 7.47–7.39 (m, 12H), 7.17–7.13 (m, 2H), 7.08–7.02 (m, 6H), 1.16 (s, 21H). <sup>13</sup>C-NMR (101 MHz, [D]Chloroform) δ = 145.71, 144.55, 132.45, 132.00, 131.40, 131.20, 131.09, 130.70, 123.50, 122.93, 121.40, 120.80, 106.64, 92.96, 90.62, 89.77, 63.98, 18.72, 11.35. HRMS (MALDI-ToF): *m/z* = [M]<sup>+</sup> calcd. for C<sub>44</sub>H<sub>41</sub>Br<sub>3</sub>Si: 834.0522, found 834.0531.

**p-[p-(Triisopropylsilylethynyl)phenylethynyl]phenyltri(p-formyl)phenylmethane (7):** In a dry, degassed 250 mL flask, **6** (2.10 g, 2.51 mmol, 1 equiv.) was dissolved in 50 mL of freshly distilled THF and cooled to -78 °C. *t*BuLi (1.7 M in pentane, 20 mL, 34.1 mmol, 13.5 equiv.) was added to the mixture and stirred for 2 hours. DMF (5 mL, 65.3 mmol, 26 equiv.) was added to the mixture which was warmed up to r.t. over 2 hours and was thereafter stirred for 2 more hours. The reaction was cautiously quenched by addition of water, the organic phase separated, and the aqueous phase extracted twice with CH<sub>2</sub>Cl<sub>2</sub>. The combined organic phase was dried with Na<sub>2</sub>SO<sub>4</sub>, and the solvent evaporated. The purification was afforded by column chromatography (c-hexane 4:1 EtOAc) to yield **7** as a yellowish solid (1.51 g, 2.20 mmol, 88 %). <sup>1</sup>H-NMR (400 MHz, [D]Chloroform) δ = 10.00 (s, 3H), 7.89–7.77 (m, 6H), 7.51–7.39 (m, 12H), 7.25–7.16 (m, 2H), 1.13 (s, 21H). <sup>13</sup>C-NMR (63 MHz, [D]Chloroform) δ = 191.43, 151.52, 144.71, 134.75, 131.99, 131.56, 131.40, 131.29, 130.64, 129.50, 123.59, 122.76, 121.89, 106.56, 93.08, 90.38, 90.11, 65.96, 18.69, 11.32. HRMS (ESI): *m/z* = [M + Na]<sup>+</sup> calcd. for C<sub>44</sub>H<sub>41</sub>Br<sub>3</sub>SiNa: 707.2952, found 707.2942.

**p-[p-(Triisopropylsilylethynyl)phenylethynyl]phenyltri(p-hydroxymethylphenyl)methane (8):** In a 100 mL flask, **7** (1.51 mg, 2.20 mmol, 1 equiv.) was dissolved in 20 mL of MeOH and 20 mL of THF and cooled to 0 °C. NaBH<sub>4</sub> (749 mg, 19.8 mmol, 9 equiv.) was added to the solution portionwise over 1 hour. The mixture was allowed to stir for 1 more hour until the reaction was quenched upon careful addition of aqueous HCl (10 %). The mixture was diluted with CH<sub>2</sub>Cl<sub>2</sub> and transferred to a separation funnel. The aqueous phase was extracted three times with CH<sub>2</sub>Cl<sub>2</sub>, the combined organic phase dried with Na<sub>2</sub>SO<sub>4</sub> and the solvent removed in vacuo. The crude product was filtered through a silica plug (c-hexane 1:1 EtOAc), to afford **8** as a yellowish solid (1.52 mg, 2.20 mmol, quant.). <sup>1</sup>H-NMR (400 MHz, [D]Chloroform): δ = 7.49–7.41 (m, 4H), 7.39–7.34 (m, 2H), 7.17 (s, 14H), 4.51 (s, 6H), 3.02–2.86 (s, 3H), 1.17 (s, 21H). <sup>13</sup>C-NMR (63 MHz, [D]Chloroform) δ = 147.23, 145.70, 138.63, 131.98, 131.37, 131.01, 130.94, 130.89, 126.45, 123.33, 123.07, 120.61, 106.69, 92.85, 91.03, 89.34, 64.57, 64.42, 18.71, 11.34. HRMS (ESI-ToF): *m/z* = [M + Na]<sup>+</sup> calcd. for C<sub>47</sub>H<sub>50</sub>NaO<sub>3</sub>Si: 713.3421, found 713.3420.

**p-[p-(Triisopropylsilylethynyl)phenylethynyl]phenyltri(p-bromomethyl)phenylmethane (2):** In a dry, degassed 100 mL flask, **8** (419 mg, 0.606 mmol, 1 equiv.) was dissolved in 10 mL of dry, degassed CH<sub>2</sub>Cl<sub>2</sub> and cooled to -10 °C. Triphenylphosphine (965 mg, 3.64 mmol, 2 equiv.) and carbon tetrabromide (1.21 g, 3.64 mmol, 2 equiv.) were added portionwise over 20 minutes. The mixture was allowed to stir 1 more hour and was then quenched by addition of saturated aqueous NaHCO<sub>3</sub>. The organic phase was separated, dried with Na<sub>2</sub>SO<sub>4</sub> and the solvent evaporated. The crude was subjected to silica plug filtration (CH<sub>2</sub>Cl<sub>2</sub>) to afford **2** as a yellowish foam (533 mg, 0.606 mmol, quant.). <sup>1</sup>H-NMR (400 MHz, [D]Chloroform): δ = 7.47–7.38 (m, 6H), 7.34–7.27 (m, 6H), 7.23–7.15 (m, 8H), 4.48 (s, 6H), 1.15 (s, 21H). <sup>13</sup>C-NMR (101 MHz, [D]Chloroform): δ = 146.46, 146.20, 135.75, 131.98, 131.38, 131.24, 131.05, 130.89, 128.53, 123.39, 123.04, 120.98, 106.66, 92.87, 90.85, 89.50, 64.53, 33.07, 18.71, 11.34. HRMS (MALDI-ToF): *m/z* = [M]<sup>+</sup> calcd. for C<sub>47</sub>H<sub>47</sub>Br<sub>3</sub>Si: 876.0992, found 876.1003.

**Ligand 1 (p-[p-(Triisopropylsilylethynyl)phenylethynyl]phenyltris{p-[(p-bis(p-tert-butyl)phenyl)(p-[(p-methylbenzyl)thio]methyl)phenyl]methyl]benzyl]thio)methyl]phenyl)methane):** In a dry, degassed 25 mL flask, **2** (28 mg, 0.032 mmol, 1 equiv.) and **3** (74 mg, 0.118 mmol, 3.7 equiv.) were dissolved in 10 mL of freshly distilled THF. In order to start the reaction, NaH (60 % dispersed in mineral oil, 40 mg, 1.0 mmol, 10 equiv.) was added. The



mixture was allowed to stir at room temperature for 15 hours after which time, the reaction was quenched upon addition of minimum amounts of water. The mixture was dried with  $\text{Na}_2\text{SO}_4$ , and the solvents evaporated to dryness. The crude was filtered through a silica plug ( $\text{CH}_2\text{Cl}_2$ ) and subjected to automated GPC (chloroform) to give an orange oil (44 mg, 0.018 mmol, 55 %).  $^1\text{H-NMR}$  (400 MHz,  $[\text{D}]\text{Chloroform}$ ):  $\delta$  = 7.44 (s, 2H), 7.43–7.33 (m, 2H), 7.26–7.20 (m, 12H), 7.19–7.08 (m, 64H), 3.61 (d,  $J$  = 5.3 Hz, 12H), 3.59 (d,  $J$  = 9.7 Hz, 12H), 2.33 (s, 9H), 1.30 (s, 54H), 1.15 (s, 21H).  $^{13}\text{C-NMR}$  (126 MHz,  $[\text{D}]\text{Chloroform}$ )  $\delta$  = 148.53, 147.28, 146.00, 145.85, 145.07, 143.67, 136.55, 135.98, 135.60, 135.41, 135.13, 131.97, 131.70, 131.37, 131.33, 131.26, 131.09, 131.01, 130.85, 130.71, 130.66, 130.57, 129.16, 128.90, 128.29, 127.95, 127.93, 124.55, 124.24, 123.28, 120.62, 106.71, 92.75, 64.33, 63.74, 35.55, 35.39, 35.26, 34.34, 31.41, 21.14, 18.71, 11.35. HRMS (MALDI-ToF):  $m/z$  =  $[\text{M} + \text{Na}]^+$  calcd. for  $\text{C}_{176}\text{H}_{188}\text{S}_6\text{Si}$ : 2544.2697, found 2544.2725.

#### Gold Nanoparticle Formation and Purification

Au NP syntheses were carried out on a 30–50  $\mu\text{mol}$  scale with respect to the Au equivalents. Tetrachloroauric acid (6 equiv., where 6 is the number of sulfur atoms in the used ligand) was dissolved in 2.0 mL of deionized water. A solution of TOAB (12 equiv.) dissolved in 2.0 mL of  $\text{CH}_2\text{Cl}_2$  was added and the two-phase mixture was stirred for 15 minutes after which time, the aqueous phase had turned colorless and the bright orange color of the organic phase indicated complete phase transfer of the gold. The ligand (1 equiv.), dissolved in 2.5 mL of  $\text{CH}_2\text{Cl}_2$ , was added to the reaction mixture which was stirred for 15 minutes, allowing the thioether moieties and the gold to pre-organize their conformation. A freshly prepared solution of sodium borohydride (48 equiv.) in 2.0 mL of water was then added quickly to the reaction mixture, reducing the gold species and thereby causing an immediate color change to dark brown. After 15 min stirring, the resulting opaque organic phase was separated from the aqueous phase via Pasteur pipette and the aqueous phase was washed three times with  $\text{CH}_2\text{Cl}_2$  and separated in the same manner. The combined organic fractions were concentrated to a volume of approximately 0.5 mL in a Falcon tube by constant bubbling of protection gas to avoid possible thermal decomposition. 35 mL of ethanol was added in order to precipitate the particles which were then centrifuged three times at during 25 minutes at 5 °C and 4000 rpm, discarding the supernatant after every centrifugation step. After redispersion in  $\text{CH}_2\text{Cl}_2$ , the Au NPs were separated from excess ligand via size-exclusion chromatography, and stored in the freezer dispersed in  $\text{CH}_2\text{Cl}_2$  at a concentration of 1 mg  $\text{mL}^{-1}$ .

#### Gold Nanoparticle Dimerization

The formation of Au NP dimers was done on a 2 mg scale with respect to **Au-1**. The acetylene-functionalized Au NPs (**Au-1-TIPS**) were dispersed in  $\text{CH}_2\text{Cl}_2$  (200  $\mu\text{L}$ ) and TBAF (1 M in THF, 50  $\mu\text{L}$ ) was added. The mixture was left stirring for 1 hour, quenched with water, extracted with dichloromethane and dried with  $\text{Na}_2\text{SO}_4$ . After filtration, the solvent was evaporated and the deprotected particles were redispersed in  $\text{CH}_2\text{Cl}_2$  (200  $\mu\text{L}$ ). TMEDA (50  $\mu\text{L}$ ) and copper(I) chloride (2 mg) were added. The dimerization reaction was left stirring for 4 hours and then quenched with a saturated aqueous solution of ammonium chloride, extracted with  $\text{CH}_2\text{Cl}_2$  and dried with  $\text{Na}_2\text{SO}_4$ . After filtration, the solution was concentrated and subjected to size-exclusion chromatography (once in  $\text{CH}_2\text{Cl}_2$  and twice in toluene). The obtained fractions were investigated by TEM on carbon-coated copper S5 grids in order to identify pure dimer fractions. 0.67 mg of dimers were obtained (34 %; with respect to **Au-1-TIPS** containing 54.7 Au atoms in average). Highly diluted solutions were used for deposition on the grids to avoid accidental

proximity of non-linked NPs. Interparticle distances were measured manually from the TEM micrographs.

#### Gold Nanoparticle Trimerization

The Au NP “click” reactions were carried out with 3 mg of Au NPs (MW 13357 g/mol [one ligand **1** with 55 Au atoms]). The acetylene-monofunctionalized Au NPs were dispersed in dichloromethane (200  $\mu\text{L}$ ) and TBAF (1 M in THF, 50  $\mu\text{L}$ ) was added. The mixture was left stirring for 1 hour and quenched with water, extracted with dichloromethane and dried with  $\text{Na}_2\text{SO}_4$ . After filtration, the solution was concentrated by vacuum at 30 °C. The dry, deprotected Au NPs were dissolved in 50  $\mu\text{L}$  dichloromethane. Corresponding to the amount of azide moieties, 0.33 equiv. 1,3,5-tris[*p*-(azidomethyl)phenyl]benzene was dissolved in 50  $\mu\text{L}$   $\text{CH}_2\text{Cl}_2$  and added to the solution. While intensely stirring,  $\text{CuSO}_4$  (20 mol-% in respect to **Au-1-TIPS** dissolved in 20  $\mu\text{L}$  water) and sodium ascorbate (30 mol-% in respect to **Au-1-TIPS** dissolved in 20  $\mu\text{L}$  water) were added. After 4 h reaction time, the mixture was extracted with dichloromethane and dried with  $\text{Na}_2\text{SO}_4$  and dried in vacuo to yield a mixture of Au NP mono-, di- and trimers. The crude was subjected to four cycles of SEC with toluene as an eluent to remove unreacted monomers. Di- and trimers were not separated. Highly diluted solutions were used for deposition on the grids to avoid accidental proximity of non-linked NPs. Interparticle distances and di- and trimerization yields were measured manually from the TEM micrographs.

#### Acknowledgments

The authors thank the Swiss National Science Foundation (Grant no. 200020\_178808) for financial support, Cedric Wobill for providing the TGA measurements, Dr. Michael Pfeffer and Dr. Heinz Nadig for measuring ESI-HRMS and the ETH Zürich MoBiAs lab for measurement of MALDI-HRMS. M. M. acknowledges support by the 111 project (90002-18011002).

**Keywords:** Gold · Nanoparticles · Monofunctionalized particles · Macromolecular ligands · Oligomers · Organic coating

- [1] M. Faraday, *Philos. Trans. R. Soc. London* **1857**, 147, 145–181.
- [2] G. Schmid, M. Bäuml, M. Geerkens, I. Heim, C. Osemann, T. Sawitowski, *Chem. Soc. Rev.* **1999**, 28, 179–185.
- [3] E. Boisselier, D. Astruc, *Chem. Soc. Rev.* **2009**, 38, 1759–1782.
- [4] P. Mulvaney, *MRS Bull.* **2001**, 26, 1009–1014.
- [5] M.-C. Daniel, D. Astruc, *Chem. Rev.* **2004**, 104, 293–346.
- [6] M. Brust, M. Walker, D. Bethell, D. J. Schiffrin, R. Whyman, *J. Chem. Soc., Chem. Commun.* **1994**, 801–802.
- [7] M. Brust, J. Fink, D. Bethell, D. J. Schiffrin, C. Kiely, *J. Chem. Soc., Chem. Commun.* **1995**, 1655–1656.
- [8] M. Bartz, J. Küther, R. Seshadri, W. Tremel, *Angew. Chem. Int. Ed.* **1998**, 37, 2466–2468; *Angew. Chem.* **1998**, 110, 2646.
- [9] W. K. Cho, J. K. Lee, S. M. Kang, Y. S. Chi, H.-S. Lee, I. S. Choi, *Chem. Eur. J.* **2007**, 13, 6351–6358.
- [10] R. Sardar, A. M. Funston, P. Mulvaney, R. W. Murray, *Langmuir* **2009**, 25, 13840–13851.
- [11] F. J. Ibañez, F. P. Zamborini, *ACS Nano* **2008**, 2, 1543–1552.
- [12] C.-C. Huang, Z. Yang, K.-H. Lee, H.-T. Chang, *Angew. Chem. Int. Ed.* **2007**, 46, 6824–6828; *Angew. Chem.* **2007**, 119, 6948–6952.
- [13] Y. Guo, Z. Wang, H. Shao, X. Jiang, *Analyst* **2011**, 137, 301–304.
- [14] L. M. Demers, C. A. Mirkin, R. C. Mucic, R. A. Reynolds, R. L. Letsinger, R. Elghanian, G. Viswanadham, *Anal. Chem.* **2000**, 72, 5535–5541.
- [15] J. J. Storhoff, A. A. Lazarides, R. C. Mucic, C. A. Mirkin, R. L. Letsinger, G. C. Schatz, *J. Am. Chem. Soc.* **2000**, 122, 4640–4650.

- [16] R. Wilson, *Chem. Commun.* **2003**, 108–109.
- [17] D. C. Hone, A. H. Haines, D. A. Russell, *Langmuir* **2003**, *19*, 7141–7144.
- [18] D. S. Seferos, D. A. Giljohann, H. D. Hill, A. E. Prigodich, C. A. Mirkin, *J. Am. Chem. Soc.* **2007**, *129*, 15477–15479.
- [19] P. Miao, Y. Tang, Z. Mao, Y. Liu, *Part. Part. Syst. Charact.* **2017**, *34*, 1600405.
- [20] D. G. Georganopoulou, L. Chang, J.-M. Nam, C. S. Thaxton, E. J. Mufson, W. L. Klein, C. A. Mirkin, *Proc. Natl. Acad. Sci. USA* **2005**, *102*, 2273–2276.
- [21] N. L. Rosi, D. A. Giljohann, C. S. Thaxton, A. K. R. Lytton-Jean, M. S. Han, C. A. Mirkin, *Science* **2006**, *312*, 1027–1030.
- [22] M. A. Homberger, U. Simon, *Phil. Trans. R. Soc. A* **2010**, *368*, 1405–1453.
- [23] P. Podsiadlo, V. A. Sinani, J. H. Bahng, N. W. S. Kam, J. Lee, N. A. Kotov, *Langmuir* **2008**, *24*, 568–574.
- [24] M.-C. Bowman, T. E. Ballard, C. J. Ackerson, D. L. Feldheim, D. M. Margolis, C. Melander, *J. Am. Chem. Soc.* **2008**, *130*, 6896–6897.
- [25] R. Costi, A. E. Saunders, U. Banin, *Angew. Chem. Int. Ed.* **2010**, *49*, 4878–4897; *Angew. Chem.* **2010**, *122*, 4996.
- [26] M. A. Mangold, M. Calame, M. Mayor, A. W. Holleitner, *ACS Nano* **2012**, *6*, 4181–4189.
- [27] J. Liao, L. Bernard, M. Langer, C. Schönenberger, M. Calame, *Adv. Mater.* **2006**, *18*, 2444–2447.
- [28] D. Huang, F. Liao, S. Moles, D. Redinger, V. Subramanian, *J. Electrochem. Soc.* **2003**, *150*, G412–G417.
- [29] J. Wang, J. Li, J. Li, F. Liu, Y. Gu, J. Fan, B. Dong, C. Wang, L. Qiu, L. Gao, et al., *Curr. Org. Chem.* **2016**, *20*, 1786–1796.
- [30] T. A. Gschneidner, Y. A. D. Fernandez, K. Moth-Poulsen, *J. Mater. Chem. C* **2013**, *1*, 7127–7133.
- [31] J. Liao, S. Blok, S. J. van der Molen, S. Diefenbach, A. W. Holleitner, C. Schönenberger, A. Vladyka, M. Calame, *Chem. Soc. Rev.* **2015**, *44*, 999–1014.
- [32] R. Wilson, *Chem. Soc. Rev.* **2008**, *37*, 2028–2045.
- [33] J. G. Worden, A. W. Shaffer, Q. Huo, *Chem. Commun.* **2004**, 518–519.
- [34] X. Liu, J. G. Worden, Q. Dai, J. Zou, J. Wang, Q. Huo, *Small* **2006**, *2*, 1126–1129.
- [35] D. Zanchet, C. M. Micheel, W. J. Parak, D. Gerion, A. P. Alivisatos, *Nano Lett.* **2001**, *1*, 32–35.
- [36] C. Krüger, S. Agarwal, A. Greiner, *J. Am. Chem. Soc.* **2008**, *130*, 2710–2711.
- [37] R. Lévy, Z. Wang, L. Duchesne, R. C. Doty, A. I. Cooper, M. Brust, D. G. Fernig, *ChemBioChem* **2006**, *7*, 592–594.
- [38] T. Peterle, A. Leifert, J. Timper, A. Sologubenko, U. Simon, M. Mayor, *Chem. Commun.* **2008**, 3438–3440.
- [39] T. Peterle, P. Ringler, M. Mayor, *Adv. Funct. Mater.* **2009**, *19*, 3497–3506.
- [40] J. P. Hermes, F. Sander, T. Peterle, C. Cioffi, P. Ringler, T. Pfohl, M. Mayor, *Small* **2011**, *7*, 920–929.
- [41] J. P. Hermes, F. Sander, T. Peterle, M. Mayor, *Chin. Int. J. Chem.* **2011**, *65*, 219–222.
- [42] M. Lehmann, E. H. Peters, M. Mayor, *Chem. Eur. J.* **2016**, *22*, 2261–2265.
- [43] M. Lehmann, E. H. Peters, M. Mayor, *Helv. Chim. Acta* **2017**, *100*, e1600395.
- [44] W. M. Pankau, K. Verbist, G. von Kiedrowski, *Chem. Commun.* **2001**, 519–520.
- [45] Y. Hosokawa, S. Maki, T. Nagata, *Bull. Chem. Soc. Jpn.* **2005**, *78*, 1773–1782.
- [46] W. M. Pankau, S. Mönninghoff, G. von Kiedrowski, *Angew. Chem. Int. Ed.* **2006**, *45*, 1889–1891; *Angew. Chem.* **2006**, *118*, 1923.
- [47] J. P. Hermes, F. Sander, T. Peterle, R. Urbani, T. Pfohl, D. Thompson, M. Mayor, *Chem. Eur. J.* **2011**, *17*, 13473–13481.
- [48] J. P. Hermes, F. Sander, U. Fluch, T. Peterle, D. Thompson, R. Urbani, T. Pfohl, M. Mayor, *J. Am. Chem. Soc.* **2012**, *134*, 14674–14677.
- [49] F. Sander, U. Fluch, J. P. Hermes, M. Mayor, *Small* **2014**, *10*, 349–359.
- [50] A. D'Aléo, R. M. Williams, F. Osswald, P. Edamana, U. Hahn, J. van Heyst, F. D. Tichelaar, F. Vögtle, L. De Cola, *Adv. Funct. Mater.* **2004**, *14*, 1167–1177.
- [51] R. McCaffrey, H. Long, Y. Jin, A. Sanders, W. Park, W. Zhang, *J. Am. Chem. Soc.* **2014**, *136*, 1782–1785.
- [52] E. H. Peters, M. Lehmann, M. Mayor, *Part. Part. Syst. Charact.* **2018**, *35*, 1800015.
- [53] T. Sakata, S. Maruyama, A. Ueda, H. Otsuka, Y. Miyahara, *Langmuir* **2007**, *23*, 2269–2272.
- [54] L. Wei, K. Padmaja, W. J. Youngblood, A. B. Lysenko, J. S. Lindsey, D. F. Bocian, *J. Org. Chem.* **2004**, *69*, 1461–1469.
- [55] L. Wei, H. Tiznado, G. Liu, K. Padmaja, J. S. Lindsey, F. Zaera, D. F. Bocian, *J. Phys. Chem. B* **2005**, *109*, 23963–23971.
- [56] H. C. Kolb, M. G. Finn, K. B. Sharpless, *Angew. Chem. Int. Ed.* **2001**, *40*, 2004–2021; *Angew. Chem.* **2001**, *113*, 2056.
- [57] H. C. Kolb, K. B. Sharpless, *Drug Discovery Today* **2003**, *8*, 1128–1137.
- [58] A. de Meijere, F. Diederich, *Metal-Catalyzed Cross-Coupling Reactions Second, Completely Revised and Enlarged Edition*, WILEY-VCH Verlag GmbH & Co. KGaA, Weinheim, **2004**.
- [59] M. M. Alvarez, J. T. Khoury, T. G. Schaaff, M. N. Shafiqullin, I. Vezmar, R. L. Whetten, *J. Phys. Chem. B* **1997**, *101*, 3706–3712.
- [60] “ImageJ,” can be found as free download under <https://imagej.net/Welcome> (accessed Jun 17, **2016**).
- [61] P. Siemsen, R. C. Livingston, F. Diederich, *Angew. Chem. Int. Ed.* **2000**, *39*, 2632–2657; *Angew. Chem.* **2000**, *112*, 2740.
- [62] A. S. Hay, *J. Org. Chem.* **1962**, *27*, 3320–3321.
- [63] T. Zaba, A. Noworolska, C. M. Bowers, B. Breiten, G. M. Whitesides, P. Cyganik, *J. Am. Chem. Soc.* **2014**, *136*, 11918–11921.
- [64] R. K. R. Jetti, F. Xue, T. C. W. Mak, A. Nangia, *J. Chem. Soc., Perkin Trans. 2* **2000**, 1223–1232.
- [65] Y. KUBO, K. Nakamura, K. Watanabe, United States Patent Application: 0090227812 - TETRAPHENYLMETHANE SKELETON-CONTAINING COMPOUND, **A1**, 20090227812.

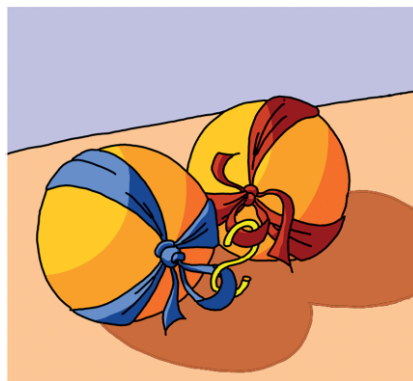
Received: March 18, 2020

**Monofunctionalized Au Nanoparticles**

*E. H. Peters, M. Mayor\** ..... 1–11



**Alkyne-Monofunctionalized Gold Nanoparticles as Massive Molecular Building Blocks**



A benzylic thioether-based ligand comprising a remote protected acetylene for the stabilization of gold nanoparticles is presented. The ligand stabilizes nanoparticles in a 1:1 ligand-to-particle ratio, affording monofunctionalized gold nanoparticles that readily undergo acetylene coupling or “click” chemistry to give nanoparticle superstructures. All synthesized structures are highly stable and withstand liquid chromatography conditions.

doi.org/10.1002/ejic.202000273